Immunity
Article

Mitochondria Are Required for Antigen-Specific T Cell Activation through Reactive Oxygen Species Signaling

Laura A. Sena,[1] Sha Li,[2] Amit Jairaman,[3] Murali Prakriya,[3] Teresa Ezponda,[1] David A. Hildeman,[5] Chyung-Ru Wang,[2] Paul T. Schumacker,[4] Jonathan D. Licht,[1] Harris Perlman,[1] Paul J. Bryce,[1] and Navdeep S. Chandel[1,*]
[1]Department of Medicine
[2]Department of Microbiology and Immunology
[3]Department of Molecular Pharmacology and Biological Chemistry
[4]Department of Pediatrics
Northwestern University Feinberg School of Medicine, Chicago, IL 60611, USA
[5]Division of Immunobiology, Department of Pediatrics, University of Cincinnati College of Medicine and Children's Hospital Medical Center, Cincinnati, OH 45229, USA
*Correspondence: nav@northwestern.edu
http://dx.doi.org/10.1016/j.immuni.2012.10.020

SUMMARY

It is widely appreciated that T cells increase glycolytic flux during activation, but the role of mitochondrial flux is unclear. Here, we have shown that mitochondrial metabolism in the absence of glucose metabolism is sufficient to support interleukin-2 (IL-2) induction. Furthermore, we used mice with reduced mitochondrial reactive oxygen species (mROS) production in T cells (T-*Uqcrfs*$^{-/-}$ mice) to show that mitochondria are required for T cell activation to produce mROS for activation of nuclear factor of activated T cells (NFAT) and subsequent IL-2 induction. These mice could not induce antigen-specific expansion of T cells in vivo, but *Uqcrfs1*$^{-/-}$ T cells retained the ability to proliferate in vivo under lymphopenic conditions. This suggests that *Uqcrfs1*$^{-/-}$ T cells were not lacking bioenergetically but rather lacked specific ROS-dependent signaling events needed for antigen-specific expansion. Thus, mitochondrial metabolism is a critical component of T cell activation through the production of complex III ROS.

INTRODUCTION

T cells orchestrate the adaptive immune response and are critical for pathogen-specific defense and immunological memory. When quiescent naive T cells are stimulated by antigen, they undergo an activation program that initiates rapid proliferation and primes them for differentiation to effector subtypes. Activation requires ligation of both the T cell receptor (TCR) and the costimulatory molecule CD28. The TCR and CD28 then initiate integrated phosphorylation-based signaling cascades that result in the activation of transcription factors, including nuclear factor of activated T cells (NFAT), activator protein 1 (AP-1), and nuclear factor of kappa light chain enhancer in B cells (NF-κB), to promote expression of proteins that drive T cell activation, such as interleukin 2 (IL-2) (Smith-Garvin et al., 2009).

A central part of the T cell activation program is a change in cellular metabolism. Proliferating cells have vastly different metabolic requirements than quiescent cells; although quiescent cells only need metabolism to support housekeeping functions and trafficking throughout the body, proliferating cells need to produce more ATP for enhanced activity, intermediates for biosynthesis, and signaling molecules to propagate anabolic metabolism.

The most dramatic change in T cell metabolism upon activation is a marked increase in glucose metabolism, which appears to be regulated by the PI3K and Akt pathway and the transcription factors Myc and ERRα (Frauwirth et al., 2002; Michalek et al., 2011; Wang et al., 2011). Activated T cells take up large amounts of glucose while simultaneously producing lactate. This has led to the widespread conceptual idea that activated T cells are primarily glycolytic despite ample oxygen supply and engage in a process termed aerobic glycolysis (Jones and Thompson, 2007; Krauss et al., 2001; Pearce, 2010; Wang et al., 1976). However, although glycolysis might be important as a rapid source of ATP and as a conduit to the pentose phosphate pathway to generate NADPH and nucleotides, it is insufficient to provide the full complement of factors needed for cell proliferation. Interestingly, T cells also increase glutamine metabolism upon activation, and glutamine is required for T cell proliferation (Carr et al., 2010). Glutamine is primarily a mitochondrial substrate in that it can fuel the mitochondrial tricarboxylic acid (TCA) cycle through conversion to α-ketoglutarate in a process called glutaminolysis. Glutaminolysis is particularly important in proliferating cells in which TCA-cycle intermediates are continually depleted for use in biosynthetic reactions (DeBerardinis et al., 2007). This suggests that mitochondrial metabolism might play an important role in T cell activation.

In addition to supporting biosynthesis, mitochondria are major sources of reactive oxygen species (ROS). Superoxide is generated at complexes I, II, and III of the mitochondrial electron transport chain (ETC) (Turrens, 2003). Complexes I and II emit superoxide into the mitochondrial matrix, where it is converted to hydrogen peroxide (H_2O_2) by superoxide dismutase 2

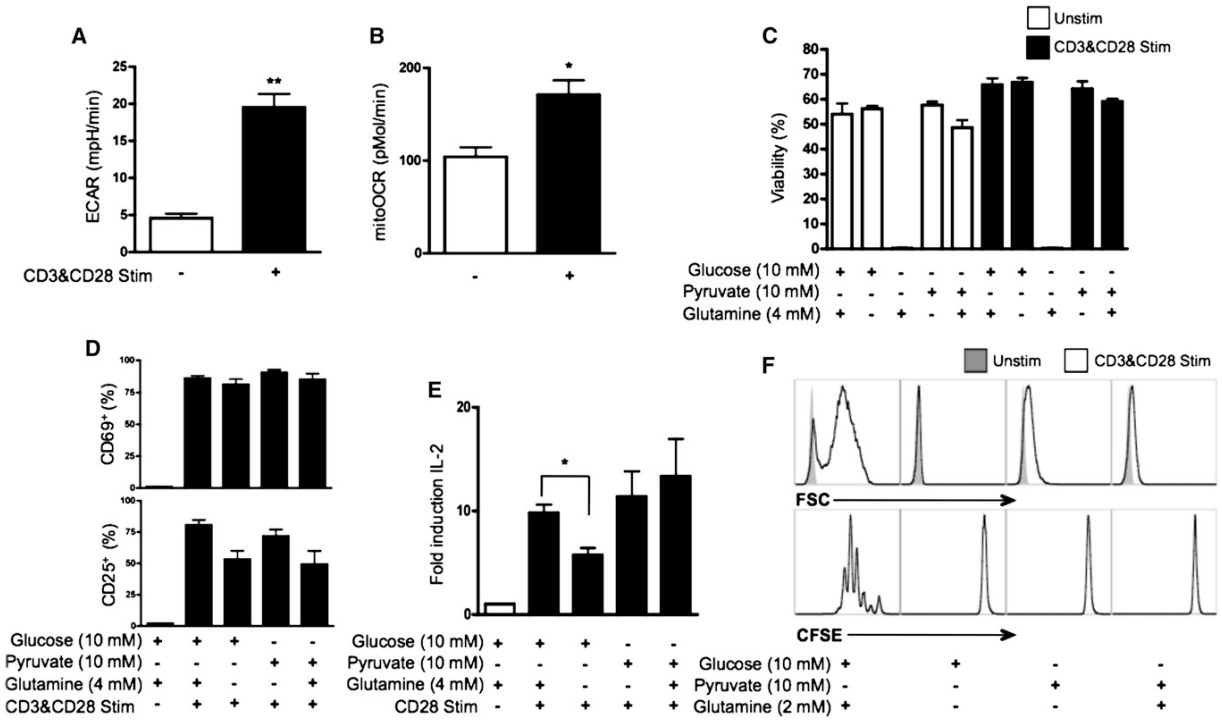

Figure 1. Mitochondrial Metabolism Is Sufficient to Support CD4+ T Cell Activation

(A and B) The extracellular acidification rate (ECAR) (A) and mitochondrial oxygen consumption rate (mitoOCR) (B) of freshly isolated CD4+ T cells and 24 hr CD3- and CD28-stimulated CD4+ T cells (n = 3 ± SEM). *p < 0.05, **p < 0.01.

(C) Cell viability of CD4+ T cells cultured in indicated media with and without CD3 and CD28 stimulation at 24 hr (n = 3 ± SEM).

(D) Surface expression of CD69 and CD25 of CD4+ T cells cultured in indicated media at 24 hr (n = 3 ± SEM).

(E) Relative IL-2 mRNA expression, normalized to ML-19 expression, of CD4+ T cells cultured in indicated media at 24 hr (n = 3 ± SEM). *p < 0.05.

(F) Cell growth (48 hr) and cell proliferation (96 hr) of CD4+ T cells cultured in indicated media (n = 3).

(SOD2). This H_2O_2 can then freely diffuse across the mitochondrial membranes into the intermembrane space and cytosol. Of note, complex III emits superoxide into both the matrix and the intermembrane space; intermembrane-space superoxide can access the cytosol through voltage-dependent anion channels without prior conversion to H_2O_2 (Han et al., 2003; Muller et al., 2004; Murphy, 2009). We and others have shown that mitochondrial ROS (mROS), particularly complex III ROS, can function as signaling intermediates (Byun et al., 2008; Schieke et al., 2008; Tormos et al., 2011; Weinberg et al., 2010). Interestingly, previous studies have shown that ROS are generated within 15 min of TCR cross-linking (Devadas et al., 2002) and that treatment of mice with panantioxidants reduces T cell expansion (Laniewski and Grayson, 2004; Piganelli et al., 2002). However, the source of these ROS and whether they are necessary for T cell activation have not previously been well defined.

Here, we report a critical role for mitochondrial metabolism in T cell activation. Mitochondrial oxygen consumption increased during T cell activation, and fueling mitochondria was sufficient to support T cell activation. mROS also increased during T cell activation, and this induction was regulated by calcium influx. Using mice with T-cell-specific reduction of Rieske iron sulfur protein (RISP), a subunit of mitochondrial complex III, we showed that mitochondrial metabolism, specifically mitochondrial complex III ROS production, is essential for T cell activation both in vitro and in vivo.

RESULTS

Mitochondrial Metabolism Can Support CD4+ T Cell Activation

In accordance with previous reports, we found that CD4+ T cells increased their extracellular acidification rate (ECAR), a lactic-acid-secretion measure indicative of the rate of glycolysis, 4-fold after 24 hr of CD3 and CD28 stimulation (Figure 1A). This phenomenon has historically eclipsed a role for mitochondria in T cell activation, yet we found that the mitochondrial oxygen consumption rate (mitoOCR) also increased after stimulation (Figure 1B). To determine whether increased glycolysis or glucose metabolism is functionally important for T cell activation, we cultured CD4+ T cells in media made with dialyzed serum with 10 mM glucose added or omitted. In the absence of glucose, nearly all unstimulated and CD3- and CD28-stimulated cells were dead after 24 hr (Figure 1C). Interestingly, cell viability could be recovered by the addition of sodium pyruvate (Figure 1C), which bypasses upstream glucose metabolism and directly fuels the mitochondrial TCA cycle (Figure S1A, available online). CD4+

T cells in pyruvate became dependent on mitochondrial metabolism, as shown by the fact that they were sensitized to cell death by treatment with mitochondrial complex I and complex III inhibitors rotenone and antimycin (Figure S1B). Furthermore, pyruvate did not rescue glucose-deprivation-induced cell death by supporting glucose metabolism through gluconeogenesis, given that the phosphoenolpyruvate carboxykinase inhibitor, 3-mercaptopropionic acid (3-MPA) had no effect on cell death (Figure S1C). Thus, mitochondrial metabolism was sufficient to support $CD4^+$ T cell viability. Of note, the presence of glutamine was insufficient to maintain T cell viability in the absence of glucose (Figure 1C); however, the downstream metabolite of glutaminolysis, α-ketoglutarate (the cell-permeable form is dimethylketoglutarate [DMK]), partially rescued cell viability (Figure S1D). This suggests that glutamine did not support viability in the absence of glucose because it failed to be converted to α-ketoglutarate, a TCA-cycle intermediate. Wellen et al. similarly describe this effect and suggest that glucose is required for glycosylation events necessary for glutamine uptake (Wellen et al., 2010).

Importantly, mitochondrial metabolism was also sufficient to support $CD4^+$ T cell activation, given that cells cultured with pyruvate or DMK in the absence of glucose upregulated surface expression of the activation markers CD69 and CD25 (Figure 1D and Figures S1E and S1F) and induced IL-2 mRNA (Figure 1E and Figure S1G) after CD3 and CD28 stimulation. Glutamine was required for full induction of IL-2 in glucose media but was not necessary for full induction of IL-2 in pyruvate media (Figure 1E). This is most likely because in the absence of glucose, pyruvate is not converted to lactate as a result of a lack of cytosolic NADH generated by glycolysis and is instead fully available for use in the TCA cycle. In the presence of glucose, NADH is generated by glycolysis, allowing for lactate dehydrogenase to convert pyruvate to lactate and NAD^+, reducing pyruvate availability to the TCA cycle and necessitating additional carbon influx through glutaminolysis (Figure S1A). The requirement of glutamine for full induction of IL-2 in glucose media might support the idea that mitochondrial metabolism is also required for T cell activation. Nevertheless, these data clearly suggest that glucose metabolism is only required for T cell activation insomuch as it can provide pyruvate to fuel the mitochondria. As previously reported, both glucose and glutamine were necessary for $CD4^+$ T cell growth and proliferation after CD3 and CD28 stimulation (Figure 1F). This was expected given that glucose and glutamine are required for biosynthesis through the pentose phosphate, hexosamine, and glutaminolysis pathways (DeBerardinis et al., 2008; Lunt and Vander Heiden, 2011; Wellen et al., 2010). The unexpected aspect of these results is that mitochondrial metabolism alone was sufficient to support T cell viability and signaling for activation prior to cell growth and proliferation.

CD3-Dependent Calcium Influx Induces mROS, which Are Required for $CD4^+$ T Cell Activation

A consequence of mitochondrial metabolism is production of mROS. Using $CD4^+$ T cells isolated from transgenic mice expressing a mitochondrial-targeted redox-sensitive GFP (mito-roGFP) (Guzman et al., 2010), we found that mROS spiked 10 min after stimulation and were maintained at a higher level than baseline through 120 min (Figure 2A). To determine whether these ROS are functionally important for T cell activation, we treated $CD4^+$ T cells with the mitochondrial-targeted antioxidant mitovitamin E (MVE). MVE is targeted to the mitochondria by covalent coupling to a triphenylphosphonium cation (TPP), which served as a control compound (Dhanasekaran et al., 2005). MVE attenuated IL-2 induction (Figure 2B) without affecting cell viability (Figure S2), indicating that mROS are necessary for T cell activation.

Interestingly, mROS induction was mediated by CD3 stimulation, not CD28 stimulation (Figure 2C). Because CD3 activation leads to rapid influx of calcium, we predicted that this calcium influx could regulate mROS induction, which also occurs early. Indeed, we found that influx of extracellular calcium was required for mROS induction, given that chelation of extracellular calcium by EDTA or inhibition of the calcium-release-activated calcium (CRAC) channel by BTP2 was sufficient to inhibit the mROS response (Figure 2D). Furthermore, influx of calcium into mitochondria was also required for mROS induction, as shown by the fact that Ruthenium Red and Ru360 also inhibited the mROS response after CD3 and CD28 stimulation (Figure 2D). It is known that several TCA-cycle enzymes are regulated by calcium (McCormack et al., 1990); thus, calcium influx into mitochondria might increase TCA cycling, electron transport, and, consequently, mitochondrial membrane potential, which is associated with increased mROS production. In support of this, we found that reduction of mitochondrial membrane potential by FCCP diminished IL-2 induction, and this defect was partially rescued by treatment with galactose oxidase (GaO) and 500 μM galactose (Gal) (Figure 2E). In the presence of Gal in the culture media, GaO produces H_2O_2, which can freely diffuse into the cell (Wang et al., 1998). Thus, calcium influx through CRAC channels and subsequent calcium influx into mitochondria increase mROS production most likely by increasing mitochondrial membrane potential, and this induction of mROS is required for T cell activation.

Mitochondrial Complex III ROS Are Required for $CD4^+$ T Cell Activation

Previous reports have indicated that the mitochondrial complex I inhibitor rotenone reduces $CD4^+$ IL-2 induction, as well as $CD8^+$ T cell blasting, proliferation, and cytokine production (Kaminski et al., 2010; Yi et al., 2006); however, inhibition of complex I coordinately reduces activity of the downstream complex III (Figure S3). Previous work in our laboratory indicated that complex III is an important source of ROS for cell signaling (Bell et al., 2007; Tormos et al., 2011; Weinberg et al., 2010). Thus, we hypothesized that complex III is the major site of mROS production in $CD4^+$ T cells. To test this, we sought to conditionally delete *Uqcrfs1* in T cells in mice. *Uqcrfs1* is the gene that encodes RISP, a complex III subunit that is required for transfer of electrons downstream of complex III and complex III ROS production (Snyder et al., 1999). Mice that possess *Uqcrfs1* flanked by loxP sites ($Uqcrfs1^{fl/fl}$) were crossed to mice that express *Cd4-cre*. Thymic cellularity (Figure 3A) and proportions and numbers of DN, DP, and SP cells (Figure 3B) were normal in $Uqcrfs1^{fl/fl}$; *Cd4-cre* mice, which permitted analysis of peripheral $CD4^+$ T cells. $CD4^+$ T cells isolated from $Uqcrfs1^{fl/fl}$; *Cd4-cre* mice had little detectable RISP by immunoblot (hereafter called

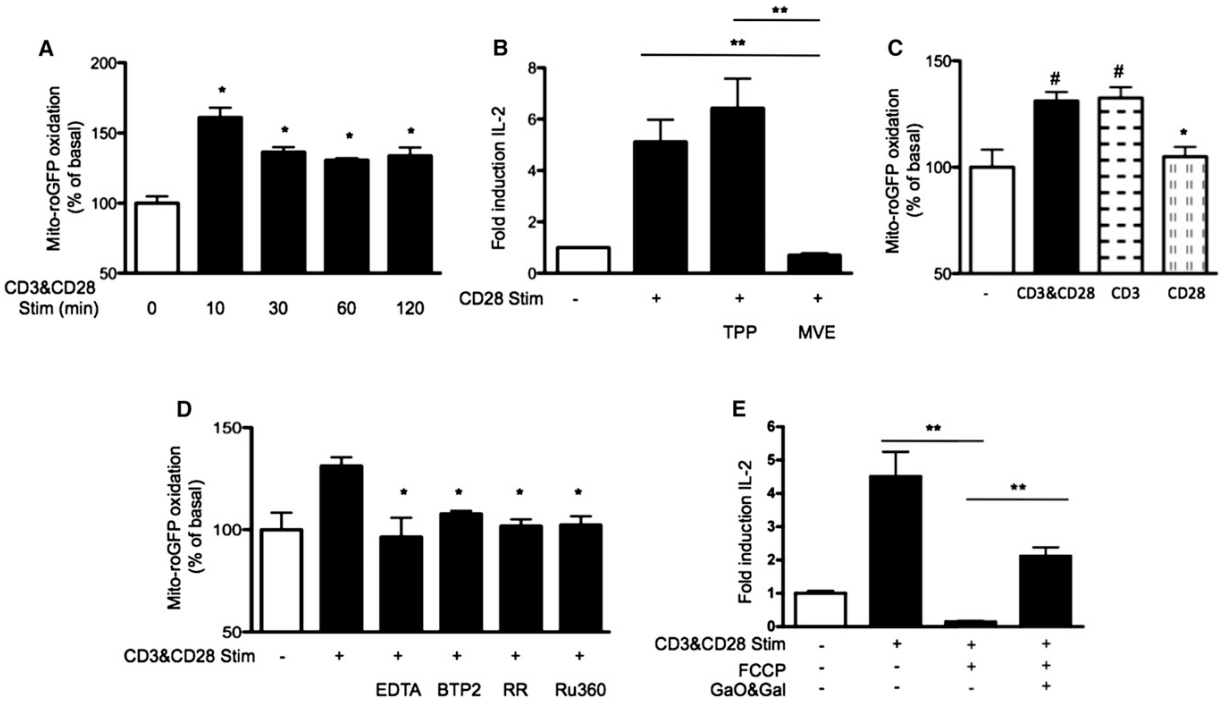

Figure 2. CD3-Dependent Calcium Influx Induces mROS, Required for T Cell Activation

(A) mROS production measured by percent oxidized mito-roGFP probe of $CD4^+$ T cells isolated from mito-roGFP transgenic mice after CD3 and CD28 stimulation ($n = 3 \pm$ SEM). *$p < 0.05$.

(B) Relative IL-2 mRNA expression, normalized to ML-19 expression, of $CD4^+$ T cells cultured with mitovitamin E (MVE) and triphenylphosphonium cation (TPP) (1.5 μM each) at 8 hr ($n = 3 \pm$ SEM). **$p < 0.01$.

(C) mROS production measured by percent oxidized mito-roGFP probe of $CD4^+$ T cells isolated from mito-roGFP transgenic mice after indicated stimulation ($n = 3 \pm$ SEM). A number sign indicates a significant difference from column 1, and an asterisk indicates a significant difference from column 2. *$p < 0.05$, #$p < 0.05$.

(D) mROS production measured by percent oxidized mito-roGFP probe of $CD4^+$ T cells isolated from mito-roGFP transgenic mice after CD3 and CD28 stimulation with calcium inhibitors (1 mM EDTA, 200 nM BTP2, 5 μm Ruthenium Red [RR], and 5 μm Ru360) ($n = 3 \pm$ SEM). **$p < 0.01$.

(E) Relative IL-2 mRNA expression, normalized to ML-19 expression, of $CD4^+$ T cells cultured with FCCP (1 μM) and GaO (0.045 U/ml) and Gal (500 μM) at 4 hr ($n = 3 \pm$ SEM). **$p < 0.01$.

Uqcrfs1$^{-/-}$ T cells or T-*Uqcrfs1*$^{-/-}$ mice), whereas non-T-cell splenocytes possessed normal amounts (Figure 3C). T-*Uqcrfs1*$^{-/-}$ mice possessed similar numbers of total splenocytes, B cells, and macrophages as *Uqcrfs1*$^{fl/fl}$ littermate controls (hereafter called WT) but showed a trend toward fewer $CD4^+$ T cells and significantly fewer $CD8^+$ T cells in the periphery (Figure 3D).

As expected, compared with WT T cells, *Uqcrfs1*$^{-/-}$ $CD4^+$ T cells produced significantly reduced amounts of activation-induced mROS as measured by MitoSOX Red (Figure 4A) and exhibited a diminished oxygen consumption rate (OCR) (Figure S4A). Surprisingly, these cells possessed a normal quantity of mitochondria, normal mitochondrial membrane potential, and a normal rate of glycolysis as determined by the ECAR (Figures S4B–S4D). Thus, we expected *Uqcrfs1*$^{-/-}$ T cells to specifically lack mitochondrial complex III ROS and mitochondrial production of ATP (oxidative phosphorylation), but not all mitochondrial function, such as orchestration of cell death. In fact, there was no change in cell viability after 24 hr of cell culture between WT $CD4^+$ T cells and *Uqcrfs1*$^{-/-}$ $CD4^+$ T cells (Figure S4E). However, *Uqcrfs1*$^{-/-}$ $CD4^+$ T cells failed to induce IL-2 (Figure 4C) and had reduced expression of activation markers CD69 and CD25 (Figure 4B) when stimulated with anti-CD3 and anti-CD28. Importantly, IL-2 induction was rescued by treatment with GaO and Gal (Figure 4C), which indicates that H_2O_2 derived from complex III is required for IL-2 induction. Further, IL-2 induction was also rescued by stimulation with PMA and ionomycin (Figure 4D), which induced mROS production (most likely at complexes I and II) to an amount comparable to that of stimulation of WT T cells with anti-CD3 and anti-CD28 (Figure 4E). IL-2 induction by PMA and ionomycin in *Uqcrfs1*$^{-/-}$ T cells was sensitive to MVE (Figure 4D), further indicating that PMA and ionomcyin stimulation could compensate for the lack of complex III ROS by inducing ROS through complexes I and II. Thus, complex III ROS are required for IL-2 induction and T cell activation.

IL-2 induction necessitates activation of the mitogen-activated protein kinase (MAPK) pathway, which has been reported to be redox sensitive (Kamata et al., 2005). However, we found that phosphorylation of extracellular-signal-regulated kinases 1 and 2 (ERK1/2) was intact after CD3 and CD28 stimulation of *Uqcrfs1*$^{-/-}$ T cells (Figure S4F). Multiple reports also suggest

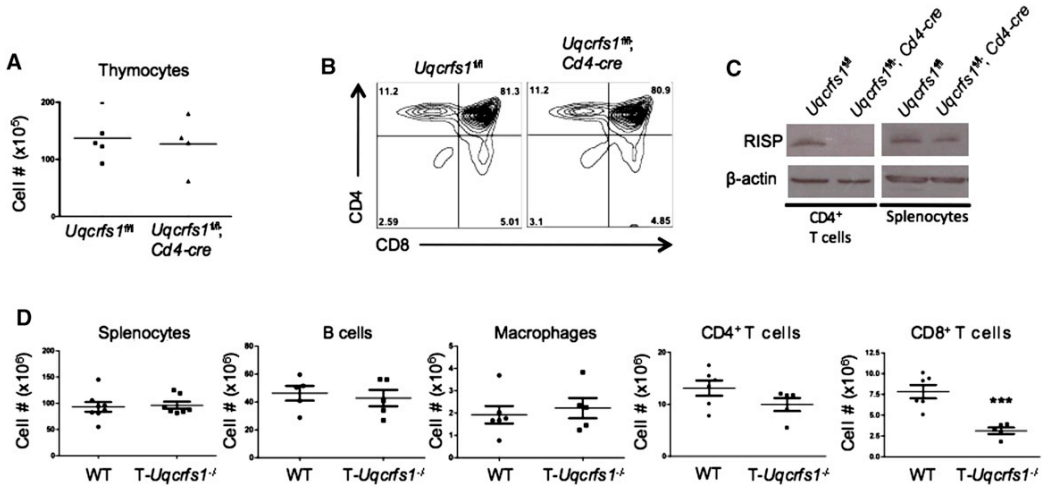

Figure 3. *Uqcrfs1*$^{fl/fl}$; *Cd4-cre* Mice Have Reduced Expression of RISP in T Cells

(A) Total number of cells isolated from mouse thymuses (n = 5 ± SEM).

(B) Surface expression of CD4 and CD8 in mouse thymus (n = 5 ± SEM).

(C) RISP expression in purified CD4$^+$ splenic T cells and total splenocytes from *Uqcrfs1*$^{fl/fl}$ and *Uqcrfs1*$^{fl/fl}$; *Cd4-cre* mice (n = 4).

(D) Total number of splenocytes (after RBC lysis), B cells (CD45$^+$B220$^+$), macrophages (CD45$^+$F4/80$^+$), CD4$^+$ T cells (CD45$^+$CD4$^+$), and CD8$^+$ T cells (CD45$^+$CD8$^+$) in *Uqcrfs1*$^{fl/fl}$ and *Uqcrfs1*$^{fl/fl}$; *Cd4-cre* spleens (n = 5–7 ± SEM). ***p < 0.001.

that NF-κB requires ROS for activation (Morgan and Liu, 2011); however, phosphorylation of IκB appeared normal in the *Uqcrfs1*$^{-/-}$ T cells (Figure S4G). Instead, we found that NFAT activation was defective in the *Uqcrfs1*$^{-/-}$ T cells—although *Uqcrfs1*$^{-/-}$ cells expressed similar quantities of cytosolic NFAT1, they failed to induce translocation of NFAT1 to the nucleus upon CD3 and CD28 stimulation (Figure 4F). To confirm this, we performed chromatin immunoprecipitation and found that NFAT1 failed to bind the IL-2 promoter upon CD3 and CD28 stimulation in *Uqcrfs1*$^{-/-}$ cells (Figure S4H). As expected, PMA and ionomycin stimulation rescued NFAT1 nuclear translocation in *Uqcrfs1*$^{-/-}$ cells (Figure S4I). Expression of the NFAT-dependent, activation-induced *il3* was diminished in *Uqcrfs1*$^{-/-}$ T cells similarly to IL-2, whereas expression of the NFAT-independent, activation-induced *myc* was unchanged (Figures S4J and S4K). Therefore, complex III ROS are required for NFAT activation.

NFAT is activated by dephosphorylation by calcineurin, which allows it to translocate to the nucleus and function as a transcription factor. Calcineurin is dependent on calcium and calmodulin; therefore, we wanted to determine whether the CRAC channel was functional in the *Uqcrfs1*$^{-/-}$ cells. We found that release of intracellular calcium stores by IP3-dependent calcium channels was normal in the *Uqcrfs1*$^{-/-}$ cells (Figure 4G, arrow), indicating that assembly and activation of the upstream TCR complex is intact in these cells. CRAC-channel activation was also intact (Figure 4G), which supports the finding that calcium influx through CRAC channels is upstream of mROS induction in T cell activation. This suggests that in T cell activation, calcium plays multiple roles, including activation of calcineurin through calmodulin and stimulation of mROS. Together, these data indicate that mitochondrial complex III ROS are required for CD4$^+$ T cell activation through NFAT in vitro.

Mitochondrial Complex III ROS Are Required for Antigen-Specific CD4$^+$ T Cell Expansion In Vivo

Uqcrfs1$^{-/-}$ CD4$^+$ T cells did not proliferate in vitro upon CD3 and CD28 stimulation or PMA and ionomycin stimulation, even with the addition of recombinant IL-2 (Figure S5). This was most likely due to an inability to generate biosynthetic intermediates that require an intact TCA cycle for their synthesis, but not due to a lack of CD25 (IL-2 receptor) surface expression, given that CD25 was reduced but not absent (Figure 4B). To determine whether *Uqcrfs1*$^{-/-}$ CD4$^+$ T cells could proliferate in vivo, we measured homeostatic expansion of purified *Uqcrfs1*$^{fl/fl}$ or *Uqcrfs1*$^{-/-}$ CD4$^+$ T cells in Rag1-deficient mice. Surprisingly, the *Uqcrfs1*$^{-/-}$ cells had no defect in homeostatic expansion (Figure 5A), suggesting that these cells met their ATP and biosynthetic demands necessary for proliferation in the in vivo environment. However, when we coinjected *Uqcrfs1*$^{fl/fl}$ or *Uqcrfs1*$^{-/-}$ T cells with congenic WT T cells, we found that under competitive conditions, *Uqcrfs1*$^{-/-}$ T cells did not proliferate as well as *Uqcrfs1*$^{fl/fl}$ T cells (Figure 5B). Interestingly, T-*Uqcrfs1*$^{-/-}$ mice possessed more naive CD4$^+$CD62L$^+$CD44$^-$ cells and fewer activated CD4$^+$CD62L$^-$CD44$^+$ cells than did their littermate controls (Figure 5C). This suggests that the *Uqcrfs1*$^{-/-}$ CD4$^+$ T cells might possess a defect in activation and antigen-specific, TCR-dependent proliferation, which could explain the decrease in abundance. To test this possibility, we immunized mice with the lymphocytic choriomeningitis virus (LCMV) peptide GP61 (amino acids 61–80 in the glycoprotein) in complete Freund's adjuvant (CFA) and used major histocompatibility complex (MHC) class II I-A^b LCMV GP61 tetramers to measure expansion of GP61-specific CD4$^+$ T cells after 6 days (Wojciechowski et al., 2006). Whereas GP61-specific CD4$^+$ T cells were observed in WT T cells, the T-*Uqcrfs1*$^{-/-}$ mice failed to induce expansion of GP61-specific CD4$^+$ T cells (Figure 5D). These data indicate

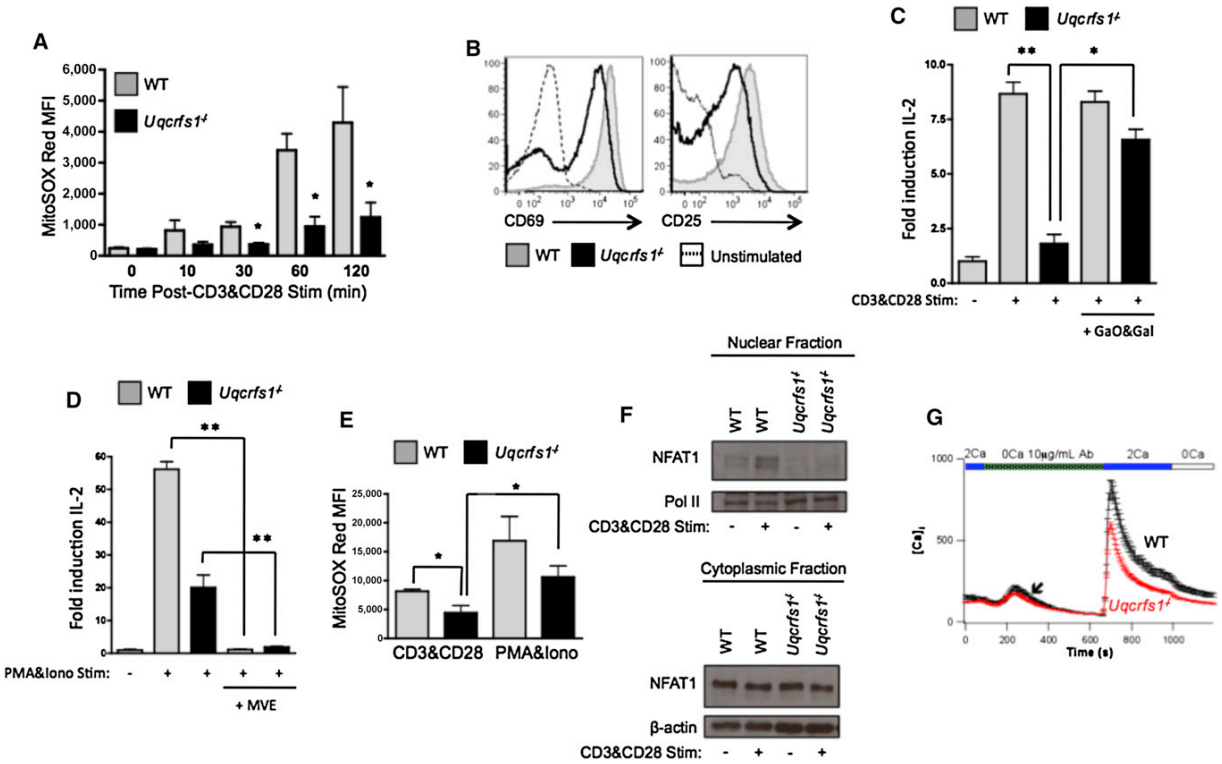

Figure 4. Mitochondrial Complex III ROS Are Required for Antigen-Specific CD4$^+$ T Cell Expansion

(A) mROS production measured by MitoSOX Red fluorescence after CD3 and CD28 stimulation (n = 3 ± SEM). *p < 0.05.

(B) Surface expression of CD69 and CD25 in CD4$^+$ T cells isolated from *Uqcrfs1*$^{fl/fl}$ and *Uqcrfs1*$^{fl/fl}$; *Cd4-cre* mice (n = 3 ± SEM).

(C) Relative IL-2 mRNA expression, normalized to ML-19 expression, of CD4$^+$ T cells isolated from *Uqcrfs1*$^{fl/fl}$ and *Uqcrfs1*$^{fl/fl}$; *Cd4-cre* mice stimulated with anti-CD3 and anti-CD28 with and without treatment with GaO (0.045 U/ml) and Gal (500 μM) (n = 2 ± SEM). p < 0.05, **p < 0.01.

(D) Relative IL-2 mRNA expression, normalized to ML-19 expression, of CD4$^+$ T cells isolated from *Uqcrfs1*$^{fl/fl}$ and *Uqcrfs1*$^{fl/fl}$; *Cd4-cre* mice stimulated with PMA and ionomycin with and without treatment with MVE (1.5 μM) (n = 3 ± SEM). **p < 0.01.

(E) mROS production measured by MitoSOX Red fluorescence (n = 4 ± SEM). *p < 0.05.

(F) Nuclear and cytosolic NFAT1 levels measured by isolation of nuclear and cytosolic lysates and then by immunoblot (n = 3).

(G) Intracellular calcium concentration measured by Fura2-AM. Cells were transferred from 2 mM calcium Ringer solution to 0 mM calcium solution with 10 μg/ml anti-CD3 for stimulation of intracellular-store release (arrow). Cells were then transferred to 2 mM calcium for store-operated calcium influx (CRAC channel influx) to occur (n = 3).

that RISP is required for antigen-specific expansion of CD4$^+$ T cells in vivo. Because the *Uqcrfs1*$^{-/-}$ CD4$^+$ T cells were capable of undergoing lymphopenia-induced homeostatic expansion in vivo, their deficiency in antigen-specific expansion was most likely due to insufficient complex III ROS generation required for T cell activation, but not to an inability to meet biosynthetic or bioenergetic demands.

Mitochondrial Complex III ROS Are Required for Antigen-Specific CD4$^+$ T Cell-Dependent Inflammation In Vivo

To determine whether deficiency of RISP in T cells would affect progression of a CD4$^+$-T-cell-dependent inflammatory disease, we assessed the susceptibility of the T-*Uqcrfs1*$^{-/-}$ mice to the ovalbumin (OVA) model of allergic asthma. In brief, T-*Uqcrfs1*$^{-/-}$ mice and littermate controls were sensitized and boosted with a mixture of OVA in alum or PBS in alum, challenged 3 weeks later with aerosolized OVA inhalation, and sacrificed for analysis of lung inflammation (Bryce et al., 2006). Lung inflammation in this model is entirely dependent on CD4$^+$ T cell function (Afshar et al., 2008). As expected, we found that the T-*Uqcrfs1*$^{-/-}$ mice did not exhibit an eosinophilic infiltrate in the bronchoalveolar lavage (BAL) fluid (Figure 6A) or signs of lung inflammation by histology (Figure 6B). Furthermore, the Th2-associated cytokines, interleukin-4 (IL-4), interleukin-5 (IL-5), and interleukin-13 (IL-13), were not increased in the lung tissue, as is typically seen in this model (Figure 6C). We also noted that the T-*Uqcrfs1*$^{-/-}$ mice failed to induce production of OVA-specific immunoglobulin E (IgE) (Figure 6D), a B cell process that requires assistance from CD4$^+$ T cells for activation and class switching.

To ensure that the T-*Uqcrfs1*$^{-/-}$ mice are capable of inducing an allergic response when T cell participation is bypassed, we administered recombinant IL-4 intratracheally for 3 days and then assessed lung inflammation. We detected an eosinophilic infiltration into the BAL fluid (Figure 6E), as well as inflammation by histology (Figure S6), in the T-*Uqcrfs1*$^{-/-}$ mice. Therefore, the

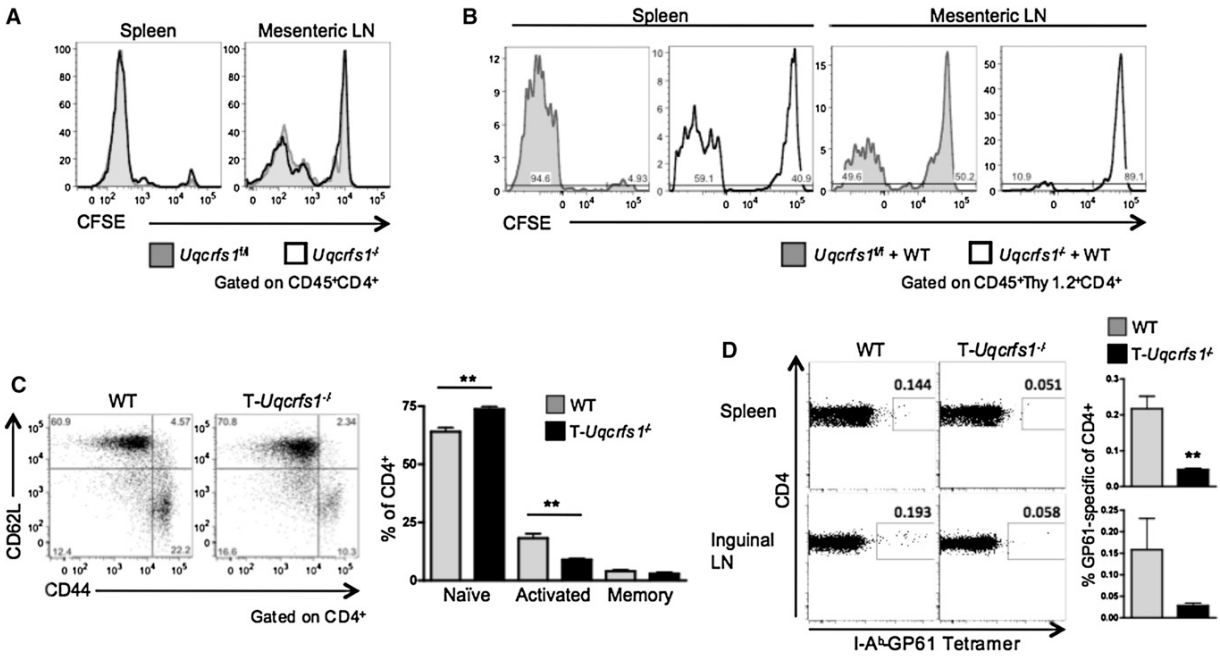

Figure 5. Mitochondrial Complex III ROS Are Required for CD4$^+$ Antigen-Specific CD4$^+$ T Cell Expansion

(A) Cell proliferation on day 4 of CD4$^+$ T cells isolated from *Uqcrfs*$^{fl/fl}$ or T-*Uqcrfs*$^{-/-}$ mice and transferred into Rag1-knockout mice (n = 3).

(B) Cell proliferation on day 4 of CD4$^+$ T cells isolated from *Uqcrfs*$^{fl/fl}$ or T-*Uqcrfs*$^{-/-}$ mice and cotransferred with Thy1.1 CD4$^+$ T cells into Rag1-knockout mice (n = 3).

(C) Surface expression of CD62L and CD44 in CD4$^+$ populations from *Uqcrfs*$^{fl/fl}$ or T-*Uqcrfs*$^{-/-}$ spleens (n = 5 ± SEM).

(D) Expansion of GP61-specific CD4$^+$ T cells 6 days after immunoprecipitation injection of GP61 peptide in CFA into *Uqcrfs1*$^{fl/fl}$ or *Uqcrfs1*$^{fl/fl}$; *Cd4-cre* mice (n = 4 ± SEM). *p < 0.05, **p < 0.01.

defect in induction of allergic asthma in the OVA model in these mice was due to dysfunctional CD4$^+$ T cells, not dysfunction of a downstream cell type. Together, these experiments suggest that RISP is required for expansion of antigen-specific CD4$^+$ T cells to promote lung inflammation.

Mitochondrial Complex III ROS Are Required for Antigen-Specific CD8$^+$ T Cell Expansion In Vivo

Given that *Cd4-cre* drives expression of Cre recombinase in both CD4$^+$ and CD8$^+$ T cells during the double-positive phase of T cell development and that we saw a decrease in numbers of CD8$^+$ T cells in the spleen (Figure 3D), we wanted to determine whether CD8$^+$ T cells also require RISP for antigen-specific expansion and function. To do this, we infected T-*Uqcrfs1*$^{-/-}$ mice with a sublethal dose of *L. monocytogenes* expressing OVA (LM-OVA). Clearance of *L. monocytogenes* after infection is mediated by T cells, and CD8$^+$ T cells provide the most substantial contribution to protective immunity (Pamer, 2004). After a primary infection, antigen-specific H2-M3-restricted T cells reach peak frequencies 5–6 days later, whereas MHC-class-Ia-restricted T cells reach peak frequencies 7–8 days after inoculation (Cho et al., 2011). Thus, we harvested splenic and hepatic leukocytes 7 days after infection and analyzed them by flow cytometry. Like CD4$^+$ T cells, the *Uqcrfs1*$^{-/-}$ CD8$^+$ T cells failed to undergo antigen-specific expansion (Figure 7A). Furthermore, when splenic and hepatic leukocytes were restimulated in vitro with OVA peptide$_{257–264}$ or heat-killed LM, very few *Uqcrfs1*$^{-/-}$ CD8$^+$ T cells produced interferon-γ (IFN-γ) (Figure 7B).

To see whether the *Uqcrfs1*$^{-/-}$ CD8$^+$ T cells could mount a memory response, we reinfected mice with LM-OVA 1 month after primary infection. We saw a robust induction of the OVA-specific CD8$^+$ T cells in the WT mice after 3 days but few in the T-*Uqcrfs1*$^{-/-}$ mice (Figure 7C). Although bacterial burden following primary infection can be regulated by the innate immune response, bacterial burden following secondary infection is more dependent on the memory T cell response. We noted that the bacterial burden in the spleen was greatly increased in the T-*Uqcrfs1*$^{-/-}$ mice, suggesting ineffective immune response and clearance of this secondary infection (Figure 7D). Thus, as for CD4$^+$ T cells, RISP is required for antigen-specific expansion of CD8$^+$ T cells.

DISCUSSION

Activated T cells have a very different metabolic profile from naive T cells. Previous studies have highlighted the critical role of increased glucose metabolism in T cell activation. In contrast, this study highlights the critical role of increased mitochondrial metabolism in T cell activation. Our results indicate that glucose metabolism only becomes important during T cell proliferation. Prior to proliferation, mitochondrial metabolism is sufficient to support cell signaling for T cell activation. Importantly, our results

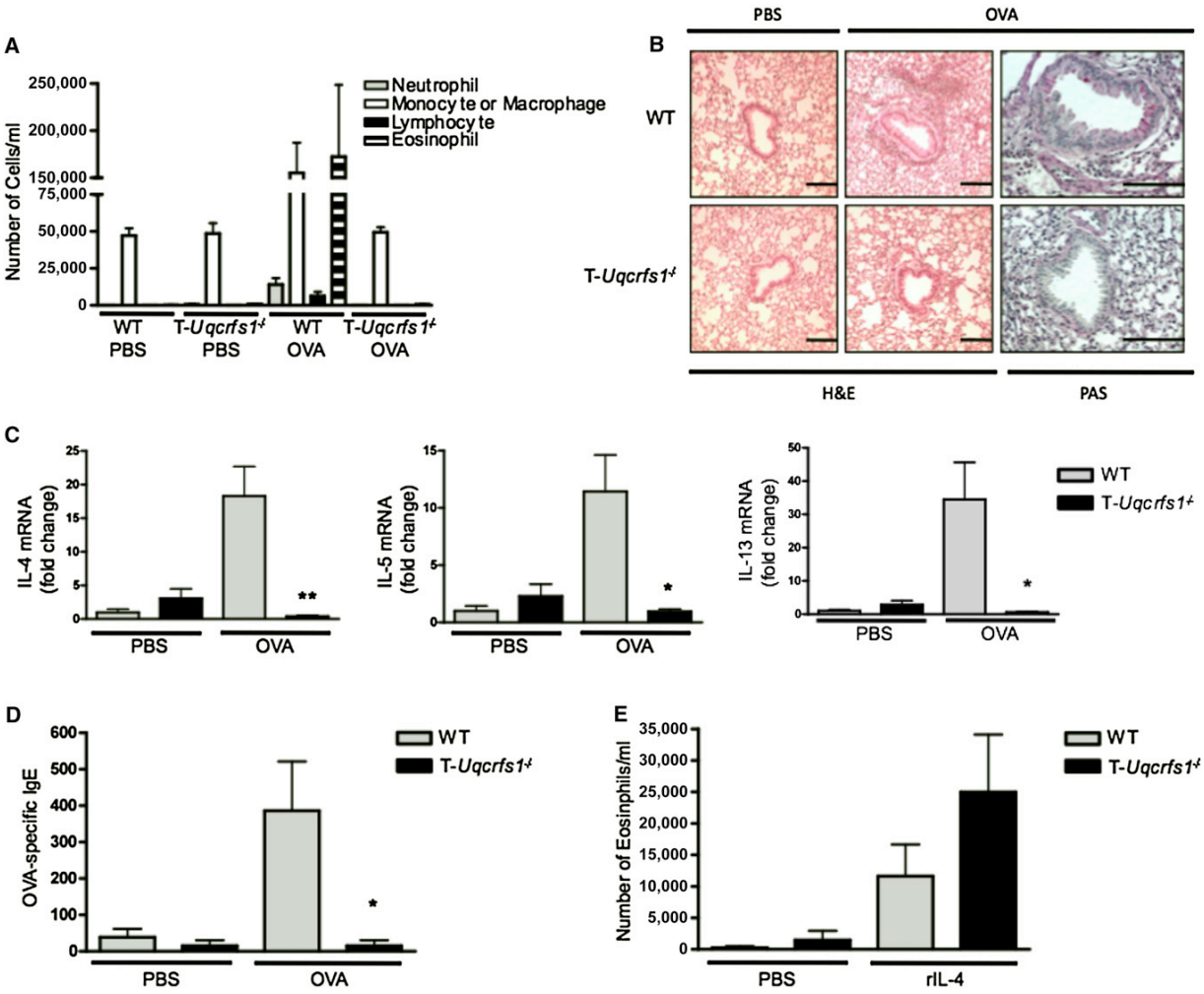

Figure 6. Mitochondrial Complex III ROS Are Required for Antigen-Specific CD4$^+$ T Cell-Dependent Inflammation In Vivo

(A–D) Ova-immunized (OVA) or sham-immunized (PBS) *Uqcrfs1*$^{fl/fl}$ and *Uqcrfs1*$^{fl/fl}$; *Cd4-cre* mice were exposed to OVA by inhalation, and airway inflammation was assessed (n = 4 ± SEM, representative of two experiments).

(A) Cellular composition of BAL fluid.

(B) Representative histological lung sections stained with hematoxylin and eosin (H&E) or PAS. The scale bars represent 100 μm.

(C) Relative IL-4, IL-5, and IL-13 mRNA expression, normalized to β-actin expression, from homogenized lungs. *$p < 0.05$, **$p < 0.01$.

(D) Serum ova-specific IgE-antibody level determined by ELISA. *$p < 0.05$.

(E) Five micrograms of recombinant mouse IL-4 or PBS was administered intranasally for 3 days, and airway inflammation was assessed. Number of eosinophils in BAL fluid (n = 5 ± SEM).

show that mROS specifically derived from complex III are required for CD4$^+$ T cell activation in vitro and antigen-specific CD4$^+$ and CD8$^+$ T cell expansion in vivo. We found that *Uqcrfs1*$^{-/-}$ T cells, which lack oxidative phosphorylation and complex III ROS production, did not express IL-2 after CD3 and CD28 stimulation in vitro. Exogenous H_2O_2 produced by the addition of GaO and Gal rescued IL-2 induction in *Uqcrfs1*$^{-/-}$ cells, and treatment of WT T cells with a mitochondrial-targeted antioxidant phenocopied *Uqcrfs1*$^{-/-}$ T cells, indicating that mROS, not oxidative phosphorylation, are necessary for T cell activation in vitro. Moreover, *Uqcrfs1*$^{-/-}$ T cells did not proliferate upon various antigen stimulations in vivo but retained the ability to proliferate under lymphopenic conditions. Thus, these cells do not possess major defects in bioenergetic or biosynthetic pathways in vivo, and we can attribute their inability to expand upon antigen stimulation in vivo to a lack of mROS for T cell activation.

Historically, mROS were thought to be primarily cytotoxic by directly damaging DNA, lipids, and proteins (Finkel and Holbrook, 2000). Recent studies have indicated that mROS are not categorically harmful and that low levels of ROS are important for healthy cell function (Sena and Chandel, 2012). This is

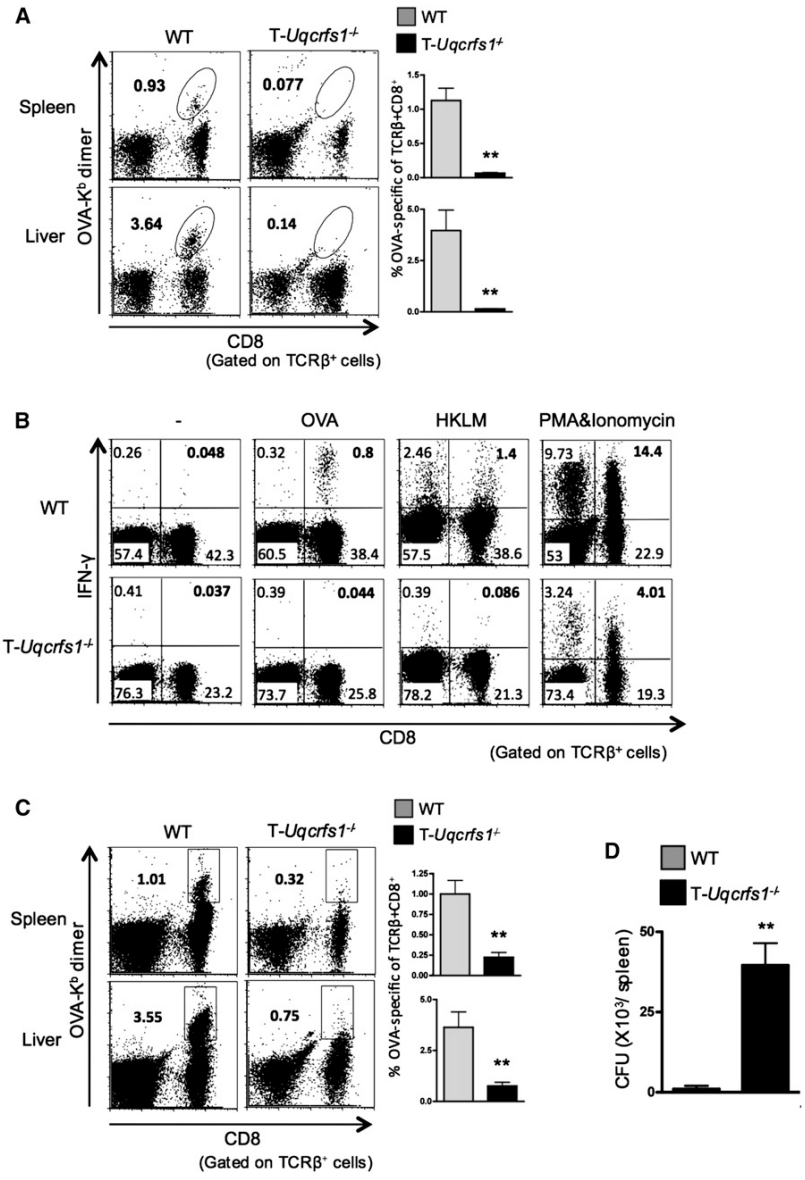

Figure 7. Mitochondrial Complex III ROS Are Required for Antigen-Specific CD8⁺ T Cell Expansion

(A) Frequency of OVA/K^b-specific $CD8^+$ T cells in LM-infected *Uqcrfs1*$^{fl/fl}$ and *Uqcrfs1*$^{fl/fl}$; *Cd4-cre* mice. *Uqcrfs*$^{fl/fl}$ and T-*Uqcrfs*$^{-/-}$ mice were infected with rLM-OVA. On day 7 postinfection, splenocytes and hepatic leukocytes were stained with anti-TCRb, anti-CD8, and OVA/K^b dimer and analyzed by flow cytometry (n = 5 ± SEM). $^{**}p < 0.01$.

(B) Frequency of OVA/K^b-specific, IFN-g–producing $CD8^+$ T cells in LM-infected *Uqcrfs1*$^{fl/fl}$ and *Uqcrfs1*$^{fl/fl}$; *Cd4-cre* mice. Splenocytes from the indicated mice were harvested on day 7 after LM infection and stimulated with either OVA peptide or heat-killed LM (HKLM). Cells were stained for CD8 expression and intracellular IFN-g and were analyzed by flow cytometry (n = 5 ± SEM).

(C) Frequency of OVA/K^b-specific $CD8^+$ T cells in *Uqcrfs1*$^{fl/fl}$ and *Uqcrfs1*$^{fl/fl}$; *Cd4-cre* mice after a second LM infection. One month after primary LM infection (2×10^3 cfu), mice were rechallenged with 4×10^4 cfu rLM-OVA. On day 3 after secondary infection, splenocytes and hepatic leukocytes were harvested and stained with anti-TCRb, anti-CD8, and OVA/K^b dimer and analyzed by flow cytometry (n = 5 ± SEM). $^{**}p < 0.01$.

(D) Bacterial burden in spleens of LM-infected *Uqcrfs1*$^{fl/fl}$ and *Uqcrfs1*$^{fl/fl}$; *Cd4-cre* mice on day 3 after secondary infection (n = 5 ± SEM). $^{**}p < 0.01$.

becoming clear in innate immunity, given that mROS appear to be essential for a wide range of innate immune function, including antiviral, antibacterial, and antiparasitic responses (West et al., 2011b). For example, West et al. recently reported that stimulation of cell-surface toll-like receptors (TLRs) leads to an increase in mROS production that is needed for clearance of *Salmonella typimurium* (West et al., 2011a). TLR signaling through mROS appears to be important in human disease because cells from individuals with TRAPS (tumor-necrosis-factor-receptor-associated periodic syndrome) exhibit greater responsiveness to LPS as a result of increased mROS production (Bulua et al., 2011). Other studies have identified a critical role for mROS in RIG-1-like receptor signaling (Tal et al., 2009) and NLRP3 inflammasome activation (Zhou et al., 2011). The present study suggests that adaptive immune cells follow suit with innate immune cells and also require mROS for activation and function.

Our results suggest that mROS induction following CD3 and CD28 stimulation of T cells is mediated by CD3-initiated calcium signaling. We found that both influx of calcium into the cytosol through CRAC channels and influx of calcium into the mitochondria are required for mROS induction. Several TCA-cycle enzymes, including pyruvate dehydrogenase and α-ketoglutarate dehydrogenase, are regulated by calcium (McCormack et al., 1990). Thus, we predict that calcium influx into mitochondria increases TCA cycling and ETC flux and consequently increases mitochondrial membrane potential and mROS production. Indeed, we show here that mitochondrial membrane potential is required for IL-2 induction through ROS. Previous studies have shown that during T cell activation, mitochondria localize to the immunological synapse, where they appear to regulate local calcium influx (Schwindling et al., 2010). This localization would also allow for the efficiency of short-lived ROS signals that are continually targeted for neutralization by antioxidant proteins, such as superoxide dismutases, catalases, glutathione, peroxiredoxins, among others.

We have identified the target of mROS to be downstream of the CRAC channel and upstream of NFAT in the calcium,

calcineurin, and NFAT pathway in T cell activation. Despite precedents in the literature for ROS regulation of NF-κB and MAPK activity, we found these pathways to be unaffected by a lack of mitochondrial complex III ROS in the present system. Given that we were able to rescue IL-2 induction in *Uqcrfs1*$^{-/-}$ T cells within 24 hr by treatment with exogenous peroxide, we suspect that mROS are required for a posttranslational protein modification rather than alteration of protein expression. Future studies will determine the specific mitochondrial complex III ROS molecular target in T cell NFAT activation. It is possible that mROS alter dephosphorylation of NFAT by calcineurin or rephosphorylation of NFAT by kinases like GSK3β to regulate the quantity of nuclear, active NFAT.

An important implication of this study is that therapeutic strategies must consider the essential role of low levels of ROS in normal physiology. We predict that antioxidant therapy or supplements might prove to be detrimental during infection because of the necessity of mROS for T cell activation.

Furthermore, this study promotes the viewpoint that cell metabolism can regulate cell function. It is clear that T cells engage in a specified or programmed change in metabolism upon antigen stimulation and do not solely exhibit homeostatic changes in metabolite flux dictated by increased demands (Jones and Thompson, 2007). This programmed change in metabolism anticipates metabolic requirements for progression to a new cell fate. For maximal efficiency, we propose that a readout of metabolism—mROS—feeds back and impinges on signaling pathways to ensure cooperation of both cellular signaling and cellular metabolism for important cell-fate decisions. Thus, cellular metabolism is not merely a structured series of reactions responsive only to energetic needs but is rather a malleable, adaptive program that is highly integrated with cell signaling. Our data indicate that mitochondria, classically known as "the powerhouse of the cell," are also signaling organelles that play a critical role in the regulation of T cell activation.

EXPERIMENTAL PROCEDURES

Animal Experiments

Animal experiments were conducted in accordance with Northwestern University's institutional guidelines on the treatment of animals.

Oxygen Consumption, Extracellular Acidification, and ROS Measurement

The OCR and ECAR were measured with the Extracellular Flux Analyzer (XF24, Seahorse Bioscience) according to the manufacturer's protocol. MitoOCR was determined by the subtraction of OCR after treatment with 2 μM rotenone (Sigma) and 2 μM antimycin (Sigma) from basal OCR. mROS production was measured either by mito-roGFP fluorescence or by MitoSOX Red (Invitrogen) fluorescence. For mito-roGFP experiments, CD4$^+$ T cells were isolated from spleens of mito-roGFP transgenic mice (gift from Paul Schumacker). Mito-roGFP contains two surface-exposed cysteine residues that can form a disulfide bond when oxidized by H_2O_2 or superoxide. Disulfide-bond formation increases the excitation spectrum peak near 400 nm at the expense of the peak near 490 nm. The ratios of fluorescence from excitation at 400 and 490 nm indicate the extent of oxidation of the probe and thus the redox potential within the mitochondrial matrix. Cells were stimulated with anti-CD3 and anti-CD28, and ratiometric measurements of excitation were taken. The mito-roGFP probe was calibrated by treatment of cells with 1 mM dithiothreitol (DTT) for complete reduction and with 1 mM t-butyl H_2O_2 for complete oxidation. The percentage of oxidized probe was determined by the following formula: % oxidized probe = (X − DTT) / (H_2O_2 − DTT). For MitoSOX Red experiments, 5 μM MitoSOX Red in complete media was added to cells at 37°C 15 min prior to harvesting. Mean fluorescence intensity was measured by flow cytometry.

Homeostatic Expansion in Rag1-Deficient Mice

CD4$^+$ T cells were purified and stained with carboxyfluorescein succinimidyl ester (CFSE), and 2 × 10^6 cells were injected retroorbitally intravenously into Rag1-deficient mice. Mice were sacrificed 4 days later, and spleens and mesenteric lymph nodes were removed for analysis by flow cytometry. For competitive homeostatic expansion, CD4$^+$ T cells were purified from both Thy1.1 mice (Jackson Laboratory) and Thy1.2, *Uqcrfs1*$^{fl/fl}$, or *Uqcrfs1*$^{fl/fl}$; *Cd4-cre* mice, stained with CFSE, and coinjected (1:1 ratio; 2 × 10^6 cells each) retroorbitally intravenously into Rag1-deficient mice.

GP61-Specific CD4$^+$ Expansion

Six- to eight-week-old mice were immunized with 150 μg GP61 peptide in CFA or CFA alone subcutaneously. Mice were sacrificed 6 days later, and spleens and inguinal lymph nodes were removed for analysis by flow cytometry (Wojciechowski et al., 2006). I-A^b-GP61 tetramer was a gift from David Hildeman.

OVA Immunization, Airway Inflammation, and Serum Antibody Levels

Four- to eight-week-old female mice were sensitized to OVA by intraperitoneal injection of 10 μg OVA (Grade VI; Sigma-Aldrich) in alum (3 mg) or alum alone at days 0 and 14. These mice were then challenged for 20 min with aerosolized 1% OVA by ultrasonic nebulization on days 21, 22, and 23 and were studied on day 24. Mice were killed, and the lungs immediately flushed with 0.8 ml BAL fluid (10% fetal calf serum, 1 mM EDTA, ×1 PBS) via the trachea. Total cells were counted, the remaining BAL fluid was cytospun onto slides, and differential cell counts were performed after staining with DiffQuik (Baxter). Tissue sections and histological staining were performed by Histo-Scientific Research Laboratories. Serum was collected on day 24, and OVA-specific IgE was determined by sandwich ELISA. OVA-specific IgE was determined by comparison with a standard curve constructed with the use of purified mouse OVA-specific IgE secreted by the hybridoma TOε.

Bacteria, Listeria Infections, and Colony Forming Unit Assays

The recombinant LM strain rLM-OVA was grown in brain-heart infusion broth supplemented with 5 μg/ml erythromycin. For primary infections, mice were intraobitally infected with 2 × 10^4 colony-forming units (cfu) of rLM-OVA. Recall infection with 4 × 10^4 cfu rLM-ova was performed 1 month after primary infection. At the indicated times after infection, mice were sacrificed and bacterial burden were determined (Dal Porto et al., 1993).

SUPPLEMENTAL INFORMATION

Supplemental Information includes Supplemental Experimental Procedures and six figures and can be found with this article online at http://dx.doi.org/10.1016/j.immuni.2012.10.020.

ACKNOWLEDGMENTS

We thank Balaraman Kalyanaraman and Joy Joseph for their kind contribution of mitovitamin E. This work was supported by National Institute of Health grants F30ES019815 (L.A.S.), T32-HL76139 (L.A.S.), 5P01HL071643 (N.S.C.), R01-AI076456 (P.B.), NS047599 (A.J.), R01-AI057753 (D.A.H.), R01-AI040310 (C.W.), RR025355 (P.T.S.), HL35440 (P.T.S.), AR050250 (H.P.), AR054796 (H.P.), AI092490 (H.P.), and HL108795 (H.P.) and funds provided by Northwestern University, Feinberg School of Medicine to Harris Perlman.

Received: May 16, 2012
Accepted: October 16, 2012
Published: February 14, 2013

REFERENCES

Afshar, R., Medoff, B.D., and Luster, A.D. (2008). Allergic asthma: a tale of many T cells. Clin. Exp. Allergy *38*, 1847–1857.

Bell, E.L., Klimova, T.A., Eisenbart, J., Moraes, C.T., Murphy, M.P., Budinger, G.R., and Chandel, N.S. (2007). The Qo site of the mitochondrial complex III is required for the transduction of hypoxic signaling via reactive oxygen species production. J. Cell Biol. *177*, 1029–1036.

Bryce, P.J., Mathias, C.B., Harrison, K.L., Watanabe, T., Geha, R.S., and Oettgen, H.C. (2006). The H1 histamine receptor regulates allergic lung responses. J. Clin. Invest. *116*, 1624–1632.

Bulua, A.C., Simon, A., Maddipati, R., Pelletier, M., Park, H., Kim, K.Y., Sack, M.N., Kastner, D.L., and Siegel, R.M. (2011). Mitochondrial reactive oxygen species promote production of proinflammatory cytokines and are elevated in TNFR1-associated periodic syndrome (TRAPS). J. Exp. Med. *208*, 519–533.

Byun, H.O., Kim, H.Y., Lim, J.J., Seo, Y.H., and Yoon, G. (2008). Mitochondrial dysfunction by complex II inhibition delays overall cell cycle progression via reactive oxygen species production. J. Cell. Biochem. *104*, 1747–1759.

Carr, E.L., Kelman, A., Wu, G.S., Gopaul, R., Senkevitch, E., Aghvanyan, A., Turay, A.M., and Frauwirth, K.A. (2010). Glutamine uptake and metabolism are coordinately regulated by ERK/MAPK during T lymphocyte activation. J. Immunol. *185*, 1037–1044.

Cho, H., Choi, H.J., Xu, H., Felio, K., and Wang, C.R. (2011). Nonconventional CD8+ T cell responses to Listeria infection in mice lacking MHC class Ia and H2-M3. J. Immunol. *186*, 489–498.

Dal Porto, J., Johansen, T.E., Catipović, B., Parfiit, D.J., Tuveson, D., Gether, U., Kozlowski, S., Fearon, D.T., and Schneck, J.P. (1993). A soluble divalent class I major histocompatibility complex molecule inhibits alloreactive T cells at nanomolar concentrations. Proc. Natl. Acad. Sci. USA *90*, 6671–6675.

DeBerardinis, R.J., Mancuso, A., Daikhin, E., Nissim, I., Yudkoff, M., Wehrli, S., and Thompson, C.B. (2007). Beyond aerobic glycolysis: transformed cells can engage in glutamine metabolism that exceeds the requirement for protein and nucleotide synthesis. Proc. Natl. Acad. Sci. USA *104*, 19345–19350.

DeBerardinis, R.J., Lum, J.J., Hatzivassiliou, G., and Thompson, C.B. (2008). The biology of cancer: metabolic reprogramming fuels cell growth and proliferation. Cell Metab. *7*, 11–20.

Devadas, S., Zaritskaya, L., Rhee, S.G., Oberley, L., and Williams, M.S. (2002). Discrete generation of superoxide and hydrogen peroxide by T cell receptor stimulation: selective regulation of mitogen-activated protein kinase activation and fas ligand expression. J. Exp. Med. *195*, 59–70.

Dhanasekaran, A., Kotamraju, S., Karunakaran, C., Kalivendi, S.V., Thomas, S., Joseph, J., and Kalyanaraman, B. (2005). Mitochondria superoxide dismutase mimetic inhibits peroxide-induced oxidative damage and apoptosis: role of mitochondrial superoxide. Free Radic. Biol. Med. *39*, 567–583.

Finkel, T., and Holbrook, N.J. (2000). Oxidants, oxidative stress and the biology of ageing. Nature *408*, 239–247.

Frauwirth, K.A., Riley, J.L., Harris, M.H., Parry, R.V., Rathmell, J.C., Plas, D.R., Elstrom, R.L., June, C.H., and Thompson, C.B. (2002). The CD28 signaling pathway regulates glucose metabolism. Immunity *16*, 769–777.

Guzman, J.N., Sanchez-Padilla, J., Wokosin, D., Kondapalli, J., Ilijic, E., Schumacker, P.T., and Surmeier, D.J. (2010). Oxidant stress evoked by pacemaking in dopaminergic neurons is attenuated by DJ-1. Nature *468*, 696–700.

Han, D., Antunes, F., Canali, R., Rettori, D., and Cadenas, E. (2003). Voltage-dependent anion channels control the release of the superoxide anion from mitochondria to cytosol. J. Biol. Chem. *278*, 5557–5563.

Jones, R.G., and Thompson, C.B. (2007). Revving the engine: signal transduction fuels T cell activation. Immunity *27*, 173–178.

Kamata, H., Honda, S., Maeda, S., Chang, L., Hirata, H., and Karin, M. (2005). Reactive oxygen species promote TNFalpha-induced death and sustained JNK activation by inhibiting MAP kinase phosphatases. Cell *120*, 649–661.

Kaminski, M.M., Sauer, S.W., Klemke, C.D., Süss, D., Okun, J.G., Krammer, P.H., and Gülow, K. (2010). Mitochondrial reactive oxygen species control T cell activation by regulating IL-2 and IL-4 expression: mechanism of ciprofloxacin-mediated immunosuppression. J. Immunol. *184*, 4827–4841.

Krauss, S., Brand, M.D., and Buttgereit, F. (2001). Signaling takes a breath—new quantitative perspectives on bioenergetics and signal transduction. Immunity *15*, 497–502.

Laniewski, N.G., and Grayson, J.M. (2004). Antioxidant treatment reduces expansion and contraction of antigen-specific CD8+ T cells during primary but not secondary viral infection. J. Virol. *78*, 11246–11257.

Lunt, S.Y., and Vander Heiden, M.G. (2011). Aerobic glycolysis: meeting the metabolic requirements of cell proliferation. Annu. Rev. Cell Dev. Biol. *27*, 441–464.

McCormack, J.G., Halestrap, A.P., and Denton, R.M. (1990). Role of calcium ions in regulation of mammalian intramitochondrial metabolism. Physiol. Rev. *70*, 391–425.

Michalek, R.D., Gerriets, V.A., Nichols, A.G., Inoue, M., Kazmin, D., Chang, C.Y., Dwyer, M.A., Nelson, E.R., Pollizzi, K.N., Ilkayeva, O., et al. (2011). Estrogen-related receptor-α is a metabolic regulator of effector T-cell activation and differentiation. Proc. Natl. Acad. Sci. USA *108*, 18348–18353.

Morgan, M.J., and Liu, Z.G. (2011). Crosstalk of reactive oxygen species and NF-κB signaling. Cell Res. *21*, 103–115.

Muller, F.L., Liu, Y., and Van Remmen, H. (2004). Complex III releases superoxide to both sides of the inner mitochondrial membrane. J. Biol. Chem. *279*, 49064–49073.

Murphy, M.P. (2009). How mitochondria produce reactive oxygen species. Biochem. J. *417*, 1–13.

Pamer, E.G. (2004). Immune responses to Listeria monocytogenes. Nat. Rev. Immunol. *4*, 812–823.

Pearce, E.L. (2010). Metabolism in T cell activation and differentiation. Curr. Opin. Immunol. *22*, 314–320.

Piganelli, J.D., Flores, S.C., Cruz, C., Koepp, J., Batinic-Haberle, I., Crapo, J., Day, B., Kachadourian, R., Young, R., Bradley, B., and Haskins, K. (2002). A metalloporphyrin-based superoxide dismutase mimic inhibits adoptive transfer of autoimmune diabetes by a diabetogenic T-cell clone. Diabetes *51*, 347–355.

Schieke, S.M., McCoy, J.P., Jr., and Finkel, T. (2008). Coordination of mitochondrial bioenergetics with G1 phase cell cycle progression. Cell Cycle *7*, 1782–1787.

Schwindling, C., Quintana, A., Krause, E., and Hoth, M. (2010). Mitochondria positioning controls local calcium influx in T cells. J. Immunol. *184*, 184–190.

Sena, L.A., and Chandel, N.S. (2012). Physiological roles of mitochondrial reactive oxygen species. Mol. Cell *48*, 158–167.

Smith-Garvin, J.E., Koretzky, G.A., and Jordan, M.S. (2009). T cell activation. Annu. Rev. Immunol. *27*, 591–619.

Snyder, C.H., Merbitz-Zahradnik, T., Link, T.A., and Trumpower, B.L. (1999). Role of the Rieske iron-sulfur protein midpoint potential in the protonmotive Q-cycle mechanism of the cytochrome bc1 complex. J. Bioenerg. Biomembr. *31*, 235–242.

Tal, M.C., Sasai, M., Lee, H.K., Yordy, B., Shadel, G.S., and Iwasaki, A. (2009). Absence of autophagy results in reactive oxygen species-dependent amplification of RLR signaling. Proc. Natl. Acad. Sci. USA *106*, 2770–2775.

Tormos, K.V., Anso, E., Hamanaka, R.B., Eisenbart, J., Joseph, J., Kalyanaraman, B., and Chandel, N.S. (2011). Mitochondrial complex III ROS regulate adipocyte differentiation. Cell Metab. *14*, 537–544.

Turrens, J.F. (2003). Mitochondrial formation of reactive oxygen species. J. Physiol. *552*, 335–344.

Wang, T., Marquardt, C., and Foker, J. (1976). Aerobic glycolysis during lymphocyte proliferation. Nature *261*, 702–705.

Wang, Y., DuBois, J.L., Hedman, B., Hodgson, K.O., and Stack, T.D. (1998). Catalytic galactose oxidase models: biomimetic Cu(II)-phenoxyl-radical reactivity. Science *279*, 537–540.

Wang, R., Dillon, C.P., Shi, L.Z., Milasta, S., Carter, R., Finkelstein, D., McCormick, L.L., Fitzgerald, P., Chi, H., Munger, J., and Green, D.R. (2011). The transcription factor Myc controls metabolic reprogramming upon T lymphocyte activation. Immunity *35*, 871–882.

Weinberg, F., Hamanaka, R., Wheaton, W.W., Weinberg, S., Joseph, J., Lopez, M., Kalyanaraman, B., Mutlu, G.M., Budinger, G.R., and Chandel, N.S. (2010). Mitochondrial metabolism and ROS generation are essential

for Kras-mediated tumorigenicity. Proc. Natl. Acad. Sci. USA *107*, 8788–8793.

Wellen, K.E., Lu, C., Mancuso, A., Lemons, J.M., Ryczko, M., Dennis, J.W., Rabinowitz, J.D., Coller, H.A., and Thompson, C.B. (2010). The hexosamine biosynthetic pathway couples growth factor-induced glutamine uptake to glucose metabolism. Genes Dev. *24*, 2784–2799.

West, A.P., Brodsky, I.E., Rahner, C., Woo, D.K., Erdjument-Bromage, H., Tempst, P., Walsh, M.C., Choi, Y., Shadel, G.S., and Ghosh, S. (2011a). TLR signalling augments macrophage bactericidal activity through mitochondrial ROS. Nature *472*, 476–480.

West, A.P., Shadel, G.S., and Ghosh, S. (2011b). Mitochondria in innate immune responses. Nat. Rev. Immunol. *11*, 389–402.

Wojciechowski, S., Jordan, M.B., Zhu, Y., White, J., Zajac, A.J., and Hildeman, D.A. (2006). Bim mediates apoptosis of CD127(lo) effector T cells and limits T cell memory. Eur. J. Immunol. *36*, 1694–1706.

Yi, J.S., Holbrook, B.C., Michalek, R.D., Laniewski, N.G., and Grayson, J.M. (2006). Electron transport complex I is required for CD8+ T cell function. J. Immunol. *177*, 852–862.

Zhou, R., Yazdi, A.S., Menu, P., and Tschopp, J. (2011). A role for mitochondria in NLRP3 inflammasome activation. Nature *469*, 221–225.